Structural insights into peptide bond formation

Jeffrey L. Hansen*, T. Martin Schmeing*, Peter B. Moore*†, and Thomas A. Steitz*†‡§

Departments of *Molecular Biophysics and Biochemistry and †Chemistry, Yale University and ‡Howard Hughes Medical Institute, 266 Whitney Avenue, New Haven, CT 06520-8114

Contributed by Thomas A. Steitz, July 8, 2002

The large ribosomal subunit catalyzes peptide bond formation and will do so by using small aminoacyl- and peptidyl-RNA fragments of tRNA. We have refined at 3-Å resolution the structures of both A and P site substrate and product analogues, as well as an intermediate analogue, bound to the *Haloarcula marismortui* 50S ribosomal subunit. A P site substrate, CCA-Phe-caproic acid–biotin, binds equally to both sites, but in the presence of sparsomycin binds only to the P site. The CCA portions of these analogues are bound identically by either the A or P loop of the 23S rRNA. Combining the separate P and A site substrate complexes into one model reveals interactions that may occur when both are present simultaneously. The α-NH_2 group of an aminoacylated fragment in the A site forms one hydrogen bond with the N3 of A2486 (2451) and may form a second hydrogen bond either with the 2′ OH of the A-76 ribose in the P site or with the 2′ OH of A2486 (2451). These interactions position the α amino group adjacent to the carbonyl carbon of esterified P site substrate in an orientation suitable for a nucleophilic attack.

Perhaps the first evolutionary event in the emergence of the "protein world" from the "RNA world" was the appearance of an enzyme capable of catalyzing peptide bond formation. The peptidyl transferase center of the large ribosomal subunit, where peptide bond synthesis occurs (1–4), has two major components: an A site, which interacts with the CCA end of aminoacylated tRNAs, and a P site, where the CCA ends of peptidyl tRNAs are bound when peptide bonds form (5–7). The reaction it catalyzes is the nucleophilic attack of the α amino group of an A site-bound aminoacyl tRNA on the carbonyl carbon of the ester bond that links a nascent peptide to a tRNA in the P site. The question we wish to address is how the ribosome, an RNA–protein machine with roots in the "RNA world," enhances the rate of peptide bond formation.

Crystal structures of the large ribosomal subunit of *Haloarcula marismortui* complexed with an analogue of peptide synthesis intermediate and an A site substrate analogue (8, 9) demonstrated that the peptidyl transferase center is composed entirely of RNA and confirmed that the CCA sequences of A and P site substrates interact with 23S rRNA in the manner deduced, in part, earlier from biochemical and genetic experiments (6, 7, 10, 11). The proximity of the N3 of A2486 (2451 in *Escherichia coli*) to the attacking α amino group and the analogue of the tetrahedral intermediate led to the suggestion that A2486 (2451) may function as a general acid/base during peptide bond formation. This hypothesis appeared to be supported by data on the pH dependence of its chemical reactivity and the finding that mutations of A2486 are dominant lethal *in vivo* (12). Further, the interaction between the N3 of A2486 (2451) and the phosphate oxygen of the reaction intermediate observed in the structure implied an altered pKa (8).

The hypothesis that A2486 (2451) is functioning as a general base has been tested most notably by its mutation to the three other nucleotides. Initial studies suggested that the impact of A2486 (2451) mutations on the rate of peptide bond formation is small, 10-fold or less (13–16). Furthermore, it is now clear that the chemical reactivity data that appeared to support the concept that A2486 (2451) acts as a general acid/base do not speak to its role in protein synthesis (17). However, more recent kinetic studies of 70S ribosomes that are greater than 90% active, done under conditions where the chemical step of peptide bond formation is likely to be rate limiting, demonstrate the existence of a titratable ribosomal component that affects catalysis and has a pKa of 7.4 (18). Its effects disappear when A2486 (2451) is mutated to U, and the rate of peptide bond formation catalyzed by the A2486U mutant ribosome is reduced by greater than 100-fold (18). These results could be explained either if A2486 (2451) acts as a general base or if there is an unknown pH-sensitive conformational change in the ribosome that depends on A2486 (2451).

Two concerns expressed about the relevance of these crystal structures to understanding the mechanism of peptide bond formation by the ribosome (19) have been shown to be unfounded (20). It has been argued that no inferences about the mechanism of peptide bond formation can be drawn from these crystal structures because large ribosomal subunits catalyze such reactions only in the presence of high concentrations of alcohol (21). Further, it has also been claimed that the ionic conditions in the crystals used to determine these structures were sufficiently far from physiological that the crystal structure is of limited functional relevance (19). However, the *H. marismortui* large subunits examined crystallographically are in fact highly active in peptide bond formation in the crystalline state, without the presence of alcohol, and manifest no sensitivity to the nature or concentration of salt (20). Furthermore, the structures obtained when peptidyl transferase substrates were diffused into preformed crystals under conditions that ensured a limited degree of reaction shows products, not substrates, bound to both the A and P sites (20). Thus, the crystal structures of the complexes previously published and those presented here are indeed relevant to the mechanism of peptide bond formation on the ribosome.

We have now determined the structure of a peptidyl-CCA bound to the P site of *H. marismortui* 50S ribosomal subunit and have refined the structures of its complexes with the substrates, products, and intermediates shown in Fig. 1. When the structures of separately determined A and P site substrate complexes are placed together in one model, we observe that the attacking α amino group of the aminoacylated A site substrate forms hydrogen bonds with the N3 of A2486 (2451) and the 2′ OH of the A76 ribose of the P site substrate. The substrates are positioned for peptide bond formation by interactions that are entirely with the RNA component of the ribosome. From the present complex structures, it appears that the only candidates for chemical assistance in catalysis, if any occurs, are the N3 of A2486 (2451) and either the 2′ OH of the P site substrate or the 2′ OH of A2486 (2451). On the basis of this alignment, we expect that the oxyanion formed in the presumed tetrahedral carbon intermediate does not interact, as suggested (8), with A2486 (2451) but more likely points in the opposite direction. In the complexes of known structure, no ribosomal component is appropriately positioned to stabilize the oxyanion, although it

Abbreviation: CCA-pcb, CCA-phenylalanine-caproic acid–biotin.

Data deposition: The atomic coordinates reported in this paper have been deposited in the Protein Data Bank, www.rcsb.org (PDB ID code 1M90).

§To whom reprint requests should be addressed. E-mail: eatherton@csb.yale.edu.

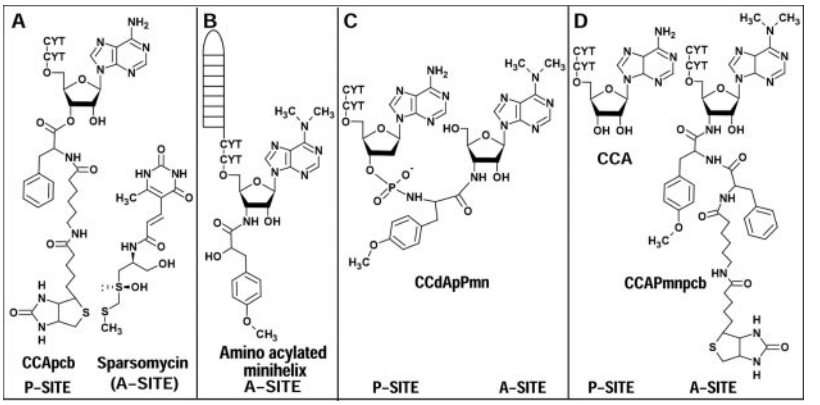

Fig. 1. Chemical structures of peptidyl transferase substrate analogues. (*A*) CCA-pcb is active as a P site substrate and binds to only the P site in the presence of the antibiotic, sparsomycin. (*B*) An aminoacylated RNA minihelix binds to the A site. (*C*) CCdA-phosphate-puromycin is an intermediate analogue containing A and P site-binding components. (*D*) CC-puromycin-phenylalanine-caproic acid–biotin and deacylated CCA are products of the peptidyl transferase reaction.

cannot be excluded that U2620 (2585) moves to do so on formation of the intermediate.

Methods

Crystals of *H. marismortui* large ribosomal subunits were grown as described (22). To prepare crystalline complexes with P site substrate, crystals were incubated in 1.6 M NaCl/30 mM $MgCl_2$/20% (vol/vol) ethylene glycol/0.5 M NH_4Cl/100 mM KOAc/12% (wt/vol) polyethylene glycol 6000, pH 6.0, at 4°C with 1 mM CCA-Phe-caproic acid–biotin (CCA-pcb) for 1 h, or with 1 mM CCA-pcb and 1 mM sparsomycin for 4 h, then flash frozen in liquid propane. Diffraction data sets were obtained by using beamline 19-ID of the Structural Biology Center at Advanced Photon Source at Argonne National Laboratory, Argonne, IL, with a 3 × 3 charge-coupled device detector, 1.033-Å wavelength, 80 × 80 μm beam size, and 0.4° oscillations. All data sets were reduced and scaled with DENZO and SCALEPACK (23). Electron density map calculations and coordinate refinement were performed by using CNS (24). The fully refined structure of the *H. marismortui* 50S at 2.4-Å resolution (Protein Data Bank ID code 1JJ2) (25), including all metals and waters, were rigid-body refined into the substrate complex data, followed by successive rounds of modeling, energy minimization, and individual B factor refinement. All modeling was done in O (26). Atomic coordinates of the 50S ribosomal subunit complexed with the sparsomycin and CCA-pcb have been deposited in the Protein Data Bank (PDB ID code 1M90).

To compare the relative positions of various substrates on the 50S subunit structures, the rRNA phosphates surrounding the peptidyl transferase center were superimposed by using the least-squares function in O. Root-mean-squared deviations between ligands were then calculated in CNS, without further superimposition of ligands, by using all corresponding RNA atoms. The theoretical transition-state model was generated by docking together the superimposed A and P site substrates, followed by rounds of modeling and Powell energy minimization with X-PLOR (27) and CNS. To fit the A and P site tRNAs from Yusopov *et al.* (28) to the CCA ligands, the 70S ribosome of *Thermus thermophilus* and the 50S subunit of *H. marismortui* were superimposed by the least-squares function in O by using phosphate atoms that surround the active site in areas where both molecules have the same overall fold. Attachment of the tRNAs to the CCAs then required some minor adjustments.

Results

We have now established the structures of two different complexes between the 50S ribosomal subunit and one analogue of a P site substrate. The substrate analogue used in both cases was a CCA sequence that is aminoacylated at its 3′ end with a phenylalanine whose α amino group is acetylated by an ε amino caproic acid molecule linked to biotin (CCA-pcb), and in the first experiment it was bound to the P site of the 50S ribosomal subunit in the presence of the antibiotic sparsomycin (Fig. 1). A difference electron density map at 3-Å resolution showed density corresponding to the CCA-Phe, which interacts with the ribosomal P loop, as well as density corresponding to the sparsomycin, which interacts extensively with the P site substrate and extends into the A site (Fig. 2*A*). In a second experiment, the CCA-pcb was soaked into crystals in the absence of sparsomycin. A difference electron density map calculated at 3-Å resolution shows clear density at a nearly equivalent level for this substrate bound at both the A and P sites (Fig. 2*B*). Refinement of the occupancy of CCA-pcb bound to both sites also shows approximately equivalent occupancy but at a level of about 50%. Both the observed one-half occupancy of each site as well as the steric overlap of the peptidyl analogue bound to these sites imply that the binding of CCA-pcb to one site precludes its binding to the second. These observations suggest that the affinities of the A and P sites for this substrate are about equal.

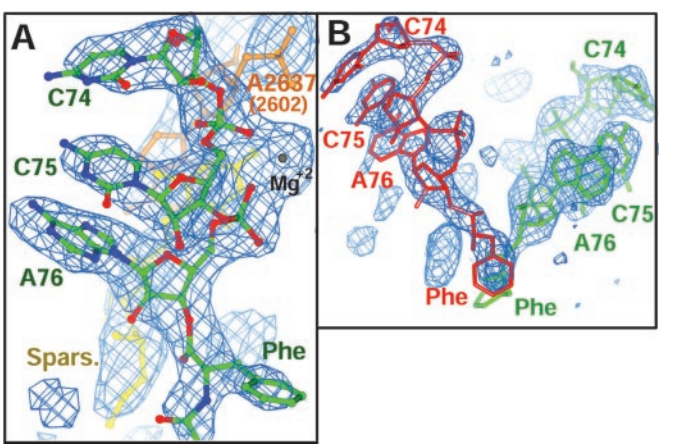

Fig. 2. Experimental electron density maps. (*A*) An $F_o - F_o$ electron density map (blue net) contoured at 4.0 σ shows density corresponding to CCA-pcb (green) in the P site and sparsomycin (yellow). Additional density corresponds to altered conformations of nucleotides such as A2637 (orange). (*B*) $F_o - F_o$ electron density map of CCA-pcb shows that in the absence of sparsomycin, the P site substrate is bound equally between the P site (green) and the A site (red).

A second P site substrate analogue that we have studied, an *N*-acetylated derivative of CC-puromycin, likewise binds in the P site in the presence of sparsomycin, but it binds only to the A site in the absence of sparsomycin. The latter result, taken together with the binding of CCA-pcb to both sites, implies that it is one or more of the methyl groups of puromycin that excludes it from the P site. In contrast, sparsomycin appears to assure complete P site binding by making interactions both with the P site substrate and the ribosome, thereby increasing P site affinity for the peptidyl-CCA.

The coordinates of 50S ribosomal subunit complexes with these two P site substrates as well as other substrate, intermediate, and product analogues (Fig. 1) have now all been refined at resolutions around 3 Å. Diffraction data for the cocrystal structure of CCA-pcb and sparsomycin extended to 2.8-Å resolution (based on I/σ of 2.0) and was 100% complete with 7.5-fold redundancy, and an average I/σ of 15.3. The free R values of these cocrystal structures are: 22.6% for CCA-pcb both with and without sparsomycin at 2.8- and 3.0-Å resolution, respectively; 26.0% for the minihelix at 3.0 Å; 22.1% for the product in the A site at 3.1 Å; and 27.6% for CCdA-phosphate-puromycin at 3.1 Å. Thus, altogether we now have three sets of coordinates for analogues interacting in the A site and four for analogues interacting in the P site.

The four P site-binding analogues all interact equivalently with the P loop of 23S rRNA and likewise the A site-binding substrate analogues interact nearly identically with the A loop of 23S rRNA. The structures of these complexes were compared by superimposing the phosphorus atoms of the 23S rRNA molecules to which they are bound. The CCA sequences of the four molecules that interact with the P site superimpose very well (rms deviation $\leq$ 0.83 Å) with the C74 and C75 bases forming Watson–Crick base pairs with G2285 (2252) and G2284 (2251), respectively, which are components of the P loop of 23S RNA. The CCA portions of the A site analogues superimpose equally well (rms deviation $\leq$ 0.74 Å) with their C75 analogues all base paired with G2588 (2553) in the A loop of 23S rRNA. In addition, the A76 analogues in all these molecules make A minor interactions with 23S rRNA sequences in both the A and P sites, as described (29).

The CCA portions of A and P site tRNA substrate analogues bind to isolated 50S subunits in a manner consistent with the model of tRNA bound to the A and P sites of 70S ribosomal subunit derived from a 5.5-Å resolution map (28). Because of the strong similarity that exists between homologous ribosomes from different species, we were able to superimpose the *H. marismortui* large ribosomal subunit structure on that of the *Thermus thermophilus* 70S ribosome (28). The A and P site tRNAs modeled into the 70S model could then be positioned in the *H. marismortui* 50S structure. The acceptor stems of ribosome-bound tRNAs protrude into the peptidyl transferase site of *H. marismortui* 50S subunit in such a way that only modest adjustments of the positions of C74 in both the A and P site-bound tRNAs are required to join them to the corresponding CCA sequences in our analogue complexes (Fig. 3). Thus, within the accuracy of coordinates derived from a 5.5-Å resolution map, the structures derived from these analogue complexes reported here are consistent with the coordinates of intact tRNA bound to eubacterial 70S ribosome.

It is important to note that, whereas the acceptor stems of the tRNAs in the A and P sites are related largely by a translation, their CCA ends, which interact with the A and P sites, are related to each other by an approximate 180° rotation (Fig. 3). The difference in the relative orientations of the CCA ends and the acceptor stems of the A and P site tRNAs is accommodated almost entirely between nucleotides 72 and 74 of the tRNA. It is possible that this difference in the acceptor end conformation may provide an energetic contribution to the translocation of the A site tRNA to the P site after peptidyl transfer (8).

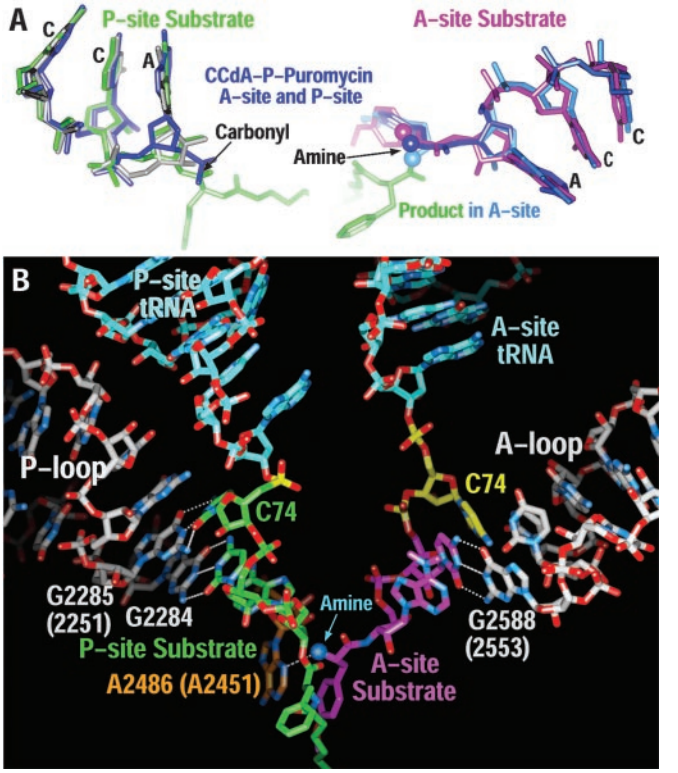

Fig. 3. The various peptidyl transferase fragment substrate and product analogues and tRNA bind the 50S and 70S ribosome in the same way. (*A*) Three P site substrate analogues, CCA-pcb (green), CC-acetylated-puromycin (gray), the CCdA portion of CCdA-phosphate-puromycin (dark blue), which results when ribosomal RNA is superimposed by least squares among the cocrystal structures. Likewise, three A site substrates, stem–loop–CC-puromycin (purple), A site product (20) (light blue and green), and puromycin from the CCdA-phosphate-puromycin (dark blue) structure also superimposed. The P and A site substrates are separated for clearer viewing. (*B*) The positions of the acceptor ends of tRNA molecules (blue backbone) bound to the A and P sites of the 70S ribosome (28) agree well with the positions of the fragment P site (green) and A site (purple) bound to the 50S subunit. A2486 (2451) is yellow.

Using the structures described here, it is also possible to construct a model for a 50S ribosomal subunit that has substrates bound to both its A and P sites. Again, this was accomplished by superimposing the 23S rRNA of the A site substrate complex on the 23S rRNA of the complex with a P site substrate and sparsomycin. In this proposed complex, which contains both substrates, the α amino group of an A site-bound aminoacyl–tRNA is held in place by hydrogen bonds that position it adjacent to the carbonyl carbon of the peptidyl ester it is to attack in the P site (Fig. 4). The α amino group is close enough to the N3 of A2486 (2451) to form a hydrogen bond, and it may also hydrogen bond either with the O2′ of A76 of the P site-bound tRNA or with the O2′ of A2486 (2451). The former possibility could explain why P site substrate analogues that contain a 2′ deoxyribose at position 76 are essentially inactive as peptidyl transferase substrates (30); however, the exact position of this 2′ OH will require the structure of a complex containing both substrates. It is important to note that in this complex, the α amino group of an A site substrate is adjacent to the carbonyl carbon of the ester bond of the peptidyl tRNA in the P site, the atom it attacks to form a new peptide bond. It would appear that only slight additional conformational changes in either the ribosome or the substrates would be required to enable the formation of a new peptide bond once substrates are bound to the ribosome, as observed. However, we cannot exclude the possibility that the

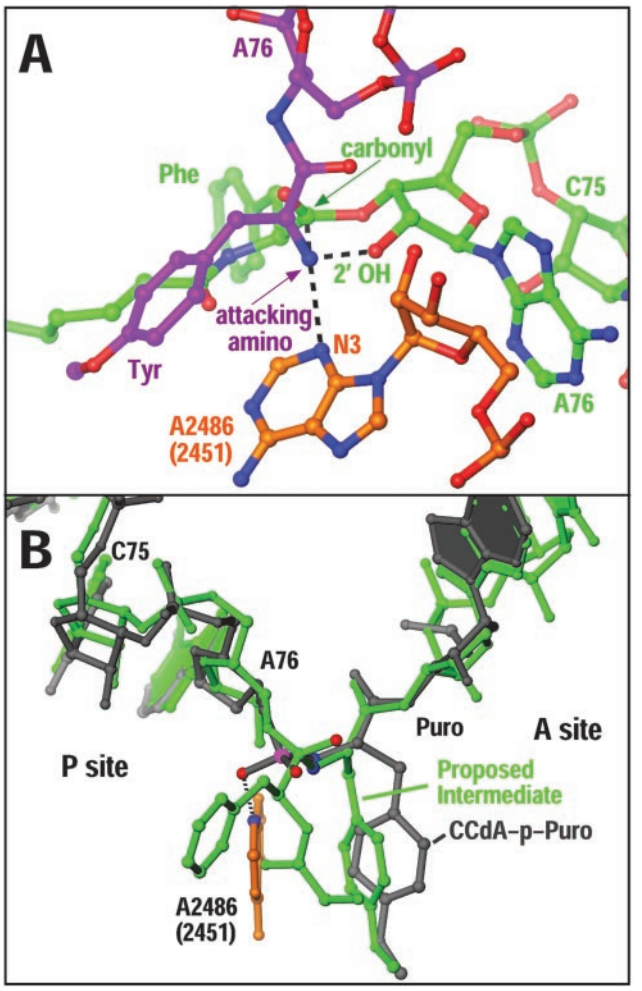

Fig. 4. A and P site substrates on the peptidyl-transferase center. (*A*) A model resulting from the superposition of the A and P site substrate complexes places the α amine of the A site substrate (purple) in position for a pro-R attack (black arrow) on the carbonyl carbon of the aminoacyl ester bond of the P site substrate (green). (*B*) The CCdAp-puromycin intermediate analogue superimposed on an intermediate modeled from the A and P site substrate complexes diverges near the tetrahedral carbon oxyanion of the intermediate.

complex formed when both substrates bind simultaneously does, indeed, have a conformation that is not seen in the separate A and P site complexes. Finally, in all of the P site substrate-like molecules examined thus far, the conformation of the ester (or amide bond) that joins its A76 analogue to the amino acid or peptide is trans; i.e., the C3′ of the A76 analogue is trans relative to the α carbon.

Discussion

Using the model proposed for the structure of the 50S subunit with both the A and P site substrates bound as well as the structure of the complex with both A and P site products bound (20), it is possible to construct a model for the trajectory of the peptide bond-forming reaction through the presumed tetrahedral intermediate (Fig. 5). The trajectory involves a pro-R nucleophilic attack of the A site α amino group on the P site carbonyl group, which should produce a tetrahedral intermediate whose oxyanion points away from the N3 of A2486 (2451). In this circumstance, the oxyanion cannot be stabilized by hydrogen bonding to the N3 of A2486 (2451), contrary to the proposal made earlier (8) on the basis of a complex with a presumed intermediate analogue, CCdA-phosphate-puromycin, a protein synthesis inhibitor devised by Welch *et al.* (31). Superposition of the Yarus inhibitor on the hypothetical tetrahedral intermediate derived from the substrates and products shows some of the significant differences at the position of the tetrahedral carbon (Fig. 5).

The concept that the oxyanion formed in the tetrahedral carbon intermediate might be stabilized by its interaction with the N3 of A2486 (2451) was derived from the structure of the subunit complex with the Yarus inhibitor (8), which was designed to be a transition-state analogue for the peptidyl transferase reaction. In this molecule, the phosphate group that links CCdA to puromycin was intended to mimic the tetrahedral carbon intermediate formed during peptide bond synthesis. It was presumed that one of its nonbridging oxygens would play the role of the oxyanion. When bound to the large ribosomal subunit, its nucleotide components interact with 23S rRNA the same way as the corresponding nucleotides in all of the other substrate-like molecules that we have examined thus far and, indeed, one of the nonbridging oxygens of the phosphate group forms a hydrogen bond with the N3 of A2486 (2451). However, as we now can see, this phosphate oxygen points in the direction opposite to that of the tetrahedral carbon oxyanion suggested by the reaction trajectory.

In addition to the phosphate being an ambiguous analogue of the tetrahedral intermediate, as noted earlier (31), there is a second structural reason to question the physiological relevance of this inhibitor structure and the phosphate oxygen hydrogen bond to the A2486 (2451). The Yarus inhibitor has a deoxyribose in the position of A76 of a P site substrate, a modification known to make a P site substrate inactive (30), and deoxyribose has a different sugar pucker from ribose (32). Thus, the placement of the phosphate group in the current refined structure of the Yarus inhibitor complex would not be possible if the deoxy-A in that molecule were replaced by the ribo-A found in all tRNA molecules. The distance between the phosphate group and the O2′ of its P site, A76 analogue, would be unacceptably short. Thus, we conclude that it is unlikely that the N3 of A2486 (2451) participates in the stabilization of the tetrahedral intermediate that forms during peptide bond synthesis by interacting with the oxyanion. Rather, such a stabilization, if it occurs, must be accomplished by another component of the active site, which is as yet unidentified. Perhaps, for example, U2620 (2585) undergoes an additional orientation change that enables it to serve this function.

Peptidyl Transferase Mechanism. It is undoubtedly the case that the major contribution to the catalytic power of the ribosome in peptide bond synthesis is provided by its ability to correctly juxtapose the two substrates, as is the case with all other enzymes (33). Correct positioning of the reactants is achieved by interactions between the acceptor ends of the A and P site-bound tRNAs and the A and P loops, respectively, as well as the interactions of the attacking α amino group of the aminoacylated tRNA in the A site with the N3 of A2486 (2451) and either the 2′ hydroxyl of the 3′ terminal ribose in the P site tRNA or the 2′ OH of A2486 (2451). The question that arises, however, is whether the ribosome further enhances the rate of peptide bond formation through chemical catalysis involving either the RNA components at the catalytic site or a bound metal ion (34). Presently, the only candidates sufficiently close to the nascent peptide bond to act as a general base/acid are A2486 (2451) or a 2′ OH group, and the only candidate for oxyanion stabilization of the tetrahedral intermediate is U2620 (2585). Electron density unambiguously identified as a metal ion has not been seen at the site of catalysis in complexes studied thus far.

We previously proposed that A2486 (2451) acts as a general base to extract a proton from the attacking α-NH_2 group to facilitate the formation of the tetrahedral intermediate (8). If this were the case, A2486 would play a role similar to that played

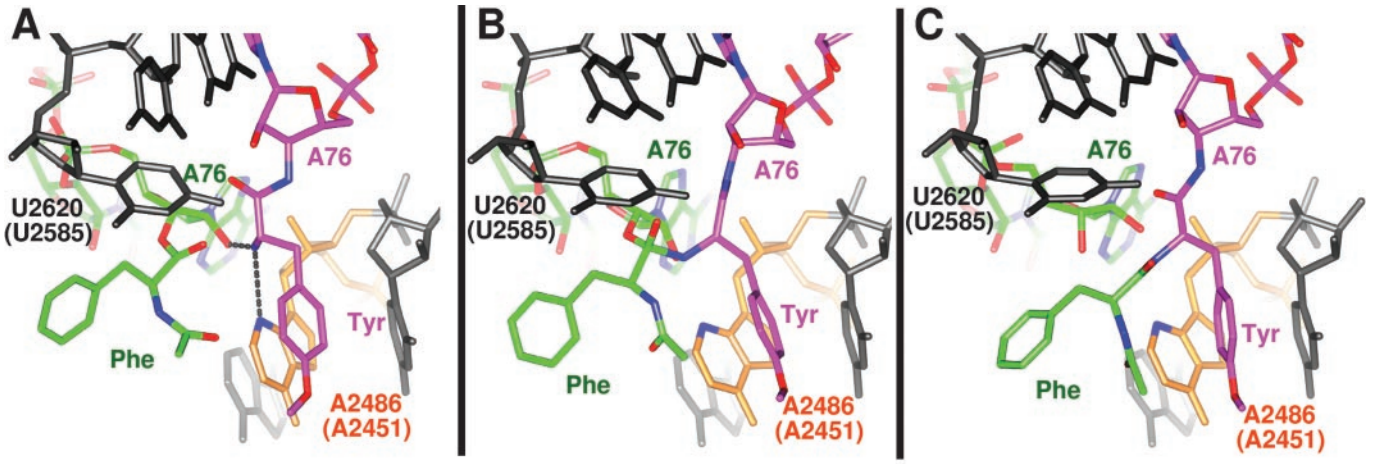

Fig. 5. Model of peptide bond formation pathway. (A theoretical model of how the peptidyl transferase reaction might proceed is illustrated in Movie 1, which is published as supporting information on the PNAS web site, www.pnas.org.) (*A*) Substrate bound at A site (purple) is in a relative position for a pro-R attack on a P site bound substrate (green), based on superposition of two cocrystal structures. (*B*) A model of the tetrahedral intermediate with the oxyanion points away from A2486 (2451). (*C*) The structure of products of the peptidyl transferase reaction bound to the peptidyl transferase center (20).

by the active site histidine in serine proteases during the deacylation step. Recent experiments using purified wild-type and mutated 70S *E. coli* ribosomes show that the change from A to U at 2451 results in a 100-fold reduction in the rate of peptide bond formation in an assay where the chemical step is likely to be rate limiting and greater than 90% of ribosomes are active (18). Furthermore, when the mutant ribosomes are assayed, the pH dependence with a pKa of 7.4 shown by wild-type ribosomes is lost. These data are consistent with the possibility that A2486 (2451) functions as a general base to enhance the rate of peptide bond formation but contributes only a 100-fold rate enhancement. Alternatively, it has been suggested that the pH dependence of peptide bond formation that has a pKa of 7.4 may arise from an essential conformational change in the ribosome that is pH dependent (18). Such a conformational alteration would also have to depend on the presence of an A at position 2486 (2451), and the explanation for such a relationship is not obvious.

Perhaps surprisingly, the role of substrate orientation played by A2486 (2451) could probably also be played to some extent by the other bases, because replacement of the A at 2486 (2451) by G, C, or U would put a hydrogen bond acceptor (N3 for G and O2 for C or U) in the same place as the N3 of A. Thus, if the bases replacing A2486 (2451) in the mutants occupy the same orientation as the wild-type A, there will be no change in the potential for hydrogen bonding with the attacking α-NH_2 group, so that the role of this base in substrate orientation may be similarly performed by any of the bases. Further, some of the hydrogen bonds between A2486 (2451) and G2482 (2447) and G2102 (2061), which in part hold A2486 (2451) in place, could still be made in A2486 (2451) mutants, although these interactions would be variable and presumably suboptimal. Substitution of A by C appears the easiest to accommodate (Fig. 6), and substitution by G the most difficult.

Site Specificity and Translocation. Aminoacylated tRNA whose α amino group is acetylated binds preferentially to the P site of 70S ribosome, whereas aminoacyl-tRNA will bind only to the A site (35). A question arises, therefore, concerning which features of the ribosome-binding sites and these tRNA substrates direct them to either the A or the P site.

Examination of the CCA-pcb substrate bound to the P site of the 50S subunit in the vicinity of the α amide of the esterified phenylalanine does not provide an unambiguous answer to why aminoacyl-tRNA with a free α-NH_2 group does not bind there. However, the α amino group would be in a somewhat hydrophobic environment with no compensatory charge or hydrogen bond acceptors provided by the ribosome. It is possible, but not certain, that the energetic cost of sequestering a free α amino group in this environment is significantly larger than that of its binding to the A site where an interaction with the N3 of A2486 is possible.

Perhaps more surprising is the observation that CCA-pcb binds equivalently to the A and P sites in the absence of the antibiotic, sparsomycin. Footprinting results from the Noller lab using 70S ribosome and tRNA substrates show that subsequent to peptide bond formation, the acceptor end of a tRNA in the A site that has just received the growing polypeptide chain moves spontaneously to the P site to give rise to what is termed a hybrid state (36, 37). However, when using small fragments derived from the acceptor end of tRNAs [such as CACCA-(AcPhe)], sparsomycin was required to footprint the fragment in the P site (7), consistent with our results. Thus, in the full 70S ribosome and using tRNA substrates, the P site would appear to have a higher affinity for peptidyl-CCA than does the A site. An

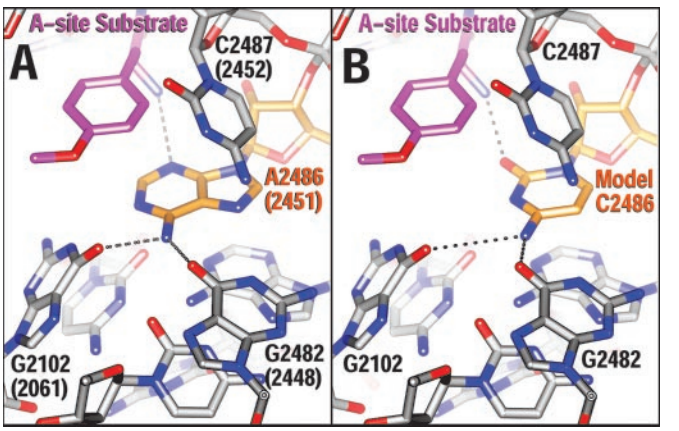

Fig. 6. Modeling of A2486 (2451) mutation to C in the A site substrate complex. (*A*) The structure of the active site shows N3 of A2486 (2451) (orange) forming a hydrogen bond (dotted line) with the attacking amine of an A site substrate (purple). (*B*) Model of mutant C2486 (2451) (orange) shows that the O2 of a C could substitute as a hydrogen bond acceptor to the α amino group, and that hydrogen bonds between the N4 of a C2486 (2451) to G2101 (2061) and G2482 (2448) might still occur.

explanation for this apparent paradox is that the context of the full tRNA is important in site selection for peptidyl-tRNA.

Because the structural relationship between the CCA and the acceptor stem of the tRNA is different in tRNAs bound to the A and P sites (Fig. 3), it is possible that the configuration exhibited by tRNA in the P site is of lower energy and thus favors binding of peptidyl tRNA to the P site. The relationship of the CCA to the acceptor stem of tRNA in the A site is rotated by 180° compared with its orientation in the P site. Perhaps the stacking interactions that occur at the junction between the CCA ends and the end of the acceptor stem of the tRNA differ sufficiently in the tRNAs bound to the two sites to explain this effect. With regard to the alternative explanation, it is not possible to evaluate whether the binding sites for the acceptor ends of tRNAs in the 70S ribosome differ from those in the isolated 50S subunit, because no independently determined structure of the 70S ribosome currently exists. The model fitted to a 5.5-Å resolution electron density map cannot establish the positions of the sugars and bases accurately enough, and so evaluation of this alternative explanation for the difference in affinity of the acceptor end of tRNA between the A and P sites must await a high-resolution crystal structure of the 70S ribosome.

Conclusion

The refined structures of substrate and product complexes with the *H. marismortui* ribosome presented here provide further insights into the possible roles played by the 23S rRNA in catalyzing peptide bond formation on the ribosome. In the present complexes, only the base of A2486 (2451) and possibly that of U2620 (2585) are close enough to the nascent peptide bond to be directly involved in the chemistry of bond formation. However, the structures of complexes with analogues of both substrates bound as well as a complex with an appropriate analogue of the tetrahedral intermediates are still required. Finally, only atomic resolution structures of the 70S ribosome complexed with aminoacyl- and peptidyl-tRNA substrates will establish whether there are any conformational differences at the peptidyl transferase site between the isolated 50S subunit and the full 70S ribosome that could account for their differing rates of peptide bond formation activity.

We thank Betty Freeborn for technical assistance with ribosome purification and crystallization, Jimin Wang for conversations about crystallography, Scott Strobel for critical comments, and Dan Klein for help with data collection. We are indebted to Andrzej Joachimiak, Ruslan (Nukri) Sanishvili, and the staff of 19-ID at the Advanced Photon Source (Argonne National Laboratory). This research was supported by National Institutes of Health Grant GM22778 and an Agouron Institute grant (to T.A.S. and P.B.M.). Use of the Argonne National Laboratory Structural Biology Center beamlines at the Advanced Photon Source was supported by the U.S. Department of Energy, Office of Biological and Environmental Research, under Contract W-31-109-ENG-38.

1. Traut, R. R. & Monro, R. E. (1964) *J. Mol. Biol.* **10,** 63–71.
2. Rychlik, I. (1966) *Biochim. Biophys. Acta* **114,** 425–427.
3. Monro, R. E. (1967) *J. Mol. Biol.* **26,** 147–151.
4. Maden, B. E., Traut, R. R. & Monro, R. E. (1968) *J. Mol. Biol.* **35,** 333–345.
5. Watson, J. D. (1964) *Bull. Soc. Chim. Biol.* **46,** 1399–1425.
6. Moazed, D. & Noller, H. F. (1989) *Cell* **57,** 585–597.
7. Moazed, D. & Noller, H. F. (1991) *Proc. Natl. Acad. Sci. USA* **88,** 3725–3728.
8. Nissen, P., Hansen, J., Ban, N., Moore, P. B. & Steitz, T. A. (2000) *Science* **289,** 920–930.
9. Ban, N., Nissen, P., Hansen, J., Moore, P. B. & Steitz, T. A. (2000) *Science* **289,** 905–920.
10. Samaha, R. R., Green, R. & Noller, H. F. (1995) *Nature (London)* **377,** 309–314.
11. Green, R., Switzer, C. & Noller, H. F. (1998) *Science* **280,** 286–289.
12. Muth, G. W., Ortoleva-Donnelly, L. & Strobel, S. A. (2000) *Science* **289,** 947–950.
13. Xiong, L., Polacek, N., Sander, P., Bottger, E. C. & Mankin, A. (2001) *RNA* **7,** 1365–1369.
14. Polacek, N., Gaynor, M., Yassin, A. & Mankin, A. S. (2001) *Nature (London)* **411,** 498–501.
15. Thompson, J., Kim, D. F., O'Connor, M., Lieberman, K. R., Bayfield, M. A., Gregory, S. T., Green, R., Noller, H. F. & Dahlberg, A. E. (2001) *Proc. Natl. Acad. Sci. USA* **98,** 9002–9007.
16. Bayfield, M. A., Dahlberg, A. E., Schulmeister, U., Dorner, S. & Barta, A. (2001) *Proc. Natl. Acad. Sci. USA* **98,** 10096–10101.
17. Muth, G. W., Chen, L., Kosek, A. B. & Strobel, S. A. (2001) *RNA* **7,** 1403–1415.
18. Katunin, V. I., Muth, G. W., Strobel, S. A., Wintermeyer, W. & Rodnina, M. V. (2002) *Mol. Cell*, in press.
19. Yonath, A. (2002) *Annu. Rev. Biophys. Biomol. Struct.* **31,** 257–273.
20. Schmeing, T. M., Seila, A. C., Hansen, J. L., Freeborn, B., Soukup, J. K., Scaringe, S. A., Strobel, S. A., Moore, P. B. & Steitz, T. A. (2002) *Nat. Struct. Biol.* **9,** 225–230.
21. Diedrich, G., Spahn, C. M., Stelzl, U., Schafer, M. A., Wooten, T., Bochkariov, D. E., Cooperman, B. S., Traut, R. R. & Nierhaus, K. H. (2000) *EMBO J.* **19,** 5241–5250.
22. Ban, N., Freeborn, B., Nissen, P., Penczek, P., Grassucci, R. A., Sweet, R., Frank, J., Moore, P. B. & Steitz, T. A. (1998) *Cell* **93,** 1105–1115.
23. Otwinowski, Z. & Minor, W. (1997) *Methods Enzymol.* **276,** 307–326.
24. Brunger, A. T., Adams, P. D., Clore, G. M., DeLano, W. L., Gros, P., Grosse-Kunstleve, R. W., Jiang, J. S., Kuszewski, J., Nilges, M., Pannu, N. S., *et al.* (1998) *Acta Crystallogr. D* **54,** 905–921.
25. Klein, D. J., Schmeing, T. M., Moore, P. B. & Steitz, T. A. (2001) *EMBO J.* **20,** 4214–4221.
26. Jones, T. A., Zou, J. Y., Cowan, S. W. & Kjeldgaard, M. (1991) *Acta Crystallogr. A* **47,** 110–119.
27. Brünger, A. T. (1992) *Nature (London)* **355,** 472–474.
28. Yusupov, M. M., Yusupova, G. Z., Baucom, A., Lieberman, K., Earnest, T. N., Cate, J. H. & Noller, H. F. (2001) *Science* **292,** 883–896.
29. Nissen, P., Ippolito, J. A., Ban, N., Moore, P. B. & Steitz, T. A. (2001) *Proc. Natl. Acad. Sci. USA* **98,** 4899–4903.
30. Quiggle, K., Kumar, G., Ott, T. A., Ryu, E. K. & Chládek, S. (1981) *Biochemistry* **20,** 3480–3485.
31. Welch, M., Chastang, J. & Yarus, M. (1995) *Biochemistry* **34,** 385–390.
32. Wahl, M. C. & Sundaralingam, M. (2000) *Nucleic Acids Res.* **28,** 4356–4363.
33. Page, M. I. & Jencks, W. P. (1971) *Proc. Natl. Acad. Sci. USA* **68,** 1678–1683.
34. Polacek, N. & Barta, A. (1998) *RNA* **4,** 1282–1294.
35. Green, R. & Noller, H. F. (1997) *Annu. Rev. Biochem.* **66,** 679–716.
36. Moazed, D. & Noller, H. F. (1989) *Nature (London)* **342,** 142–148.
37. Wilson, K. S. & Noller, H. F. (1998) *Cell* **92,** 337–349.